## Title

Evidence TRPV4 contributes to mechanosensitive ion channels in mouse skeletal muscle fibers



## Journal

Channels, 6(4)

## ISSN

1933-6950

## Authors

Ho, Tiffany C
Horn, Natalie A
Huynh, Tuan
et al.

## Publication Date

2012-07-01

## DOI

10.4161/chan.20719

Peer reviewed

Channels 6:4, 246-254; July/August 2012; © 2012 Landes Bioscience

# Evidence TRPV4 contributes to mechanosensitive ion channels in mouse skeletal muscle fibers

Tiffany C. Ho, Natalie A. Horn, Tuan Huynh, Lucy Kelava, and Jeffry B. Lansman*

Department of Cellular and Molecular Pharmacology; School of Medicine; University of California, San Francisco; San Francisco, CA USA

**Keywords:** mechanosensitive channel, skeletal muscle, muscular dystrophy, TRPV4, calcium

We recorded the activity of single mechanosensitive (MS) ion channels from membrane patches on single muscle fibers isolated from mice. We investigated the actions of various TRP (transient receptor potential) channel blockers on MS channel activity. 2-aminoethoxydiphenyl borate (2-APB) neither inhibited nor facilitated single channel activity at submillimolar concentrations. The absence of an effect of 2-APB indicates MS channels are not composed purely of TRPC or TRPV1, 2 or 3 proteins. Exposing patches to 1-oleolyl-2-acetyl-sn-glycerol (OAG), a potent activator of TRPC channels, also had no effect on MS channel activity. In addition, flufenamic acid and spermidine had no effect on the activity of single MS channels. By contrast, SKF-96365 and ruthenium red blocked single-channel currents at micromolar concentrations. SKF-96365 produced a rapid block of the open channel current. The blocking rate depended linearly on blocker concentration, while the unblocking rate was independent of concentration, consistent with a simple model of open channel block. A fit to the concentration-dependence of block gave $k_{on}$ = 13 x $10^6$ $M^{-1}s^{-1}$ and $k_{off}$ = 1609 $sec^{-1}$ with $K_D$ = ~124 μM. Block by ruthenium red was complex, involving both reduction of the amplitude of the single-channel current and increased occupancy of subconductance levels. The reduction in current amplitude with increasing concentration of ruthenium red gave a $K_D$ = ~49 μM. The high sensitivity of MS channels to block by ruthenium red suggests MS channels in skeletal muscle contain TRPV subunits. Recordings from skeletal muscle isolated from TRPV4 knockout mice failed to show MS channel activity, consistent with a contribution of TRPV4. In addition, exposure to hypo-osmotic solutions increases opening of MS channels in muscle. Our results provide evidence TRPV4 contributes to MS channels in skeletal muscle.

## Introduction

The ability to sense and respond to mechanical forces is a fundamental property of all living organisms, but remains the least understood of all sensory processes. Mechanosensitive (MS) ion channels are likely to function as the primary molecular transducers for sensing touch, distension, shear stress and osmotic gradients in vertebrate and other animal cells.[1] There is a large and growing body of research showing that alterations in intracellular and/or extracellular proteins that contribute to membrane mechanical properties can give rise to defects in mechanotransduction that alter intracellular signaling pathways. Mechanotransduction defects contribute to the pathogenesis of various diseases including cardiac hypertrophy, muscular dystrophy, kidney disease, glaucoma, and cancer.[2]

Duchenne muscular dystrophy (DMD) is a devastating and tragic genetic disease affecting 1 in 3,500 male births. DMD is caused by an absence of the cytoskeletal protein, dystrophin, which is held tightly to the sarcolemma by a glycoprotein complex in normal muscle.[3] The glycoprotein complex binds to laminin in the extracellular basement membrane and provides a link between the intracellular actin-based cytoskeleton and extracellular matrix. The structure and localization of this complex suggest it plays a role in stabilizing the surface membrane from the forces developed during muscle contraction. Although the molecular basis of DMD is well understood, there is still considerable uncertainty as to how an absence of dystrophin causes muscle degeneration.

Studies of the pathogenesis of muscular dystrophy have made use of the *mdx* mouse, a mouse model for human DMD that lacks full-length dystrophin.[4,5] Recordings of single-channel activity from skeletal muscle isolated from *mdx* mice showed dystrophin-deficiency to be associated with increased activity of MS channels.[6-9] In support of a role of MS channels in the pathogenesis of dystrophin-deficiency, pharmacological inhibitors of MS channels block an early rise in resting $[Ca^{2+}]_i$ in *mdx* muscle fibers produced in response to mechanical stress.[10] In addition, exposing muscle fibers to specific MS channel antagonists prevents contraction induced membrane damage,[11] suggesting that abnormal MS channel activity is an early event responsible for pathogenic $Ca^{2+}$ entry.

Interest has focused on identifying the proteins that contribute to MS channels in skeletal muscle. The family of TRP cation channels is widely expressed in virtually all cell types. Several TRP channels have been shown to be sensitive to mechanical stimulation, including TRPC1 and 6, TRPV2 and 4, TRPM3,

*Correspondence to: Jeffry B. Lansman; Email: jeff.lansman@ucsf.edu
Submitted: 04/17/12; Revised: 05/09/12; Accepted: 05/10/12
http://dx.doi.org/10.4161/chan.20719

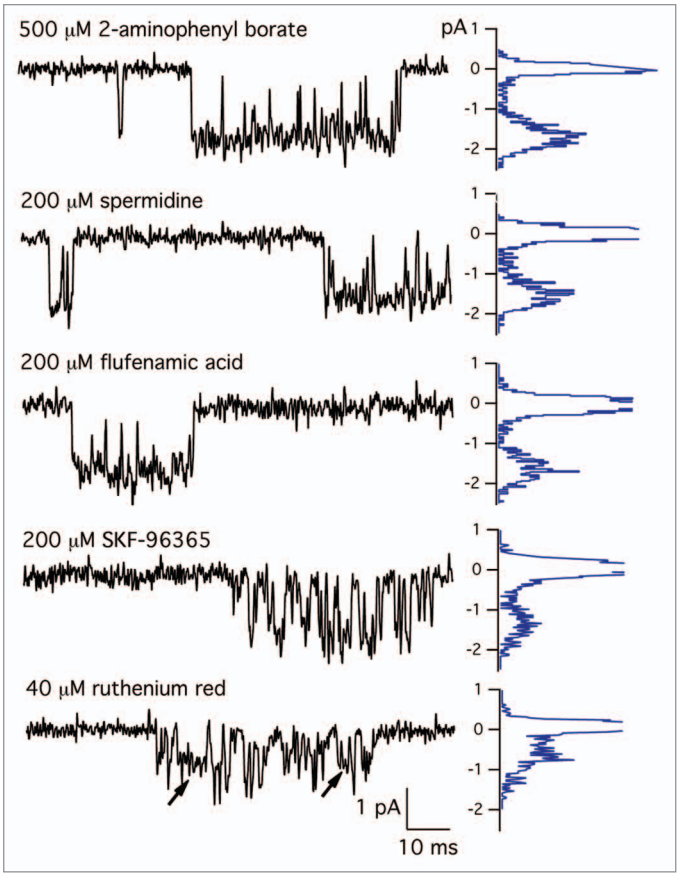


**Figure 1.** Effects of TRP channel blockers on MS channels. (Top) MS channel currents recorded with a patch electrode containing physiological saline (control) or physiological saline containing either 1000 μM 2-APB, 40 μM ruthenium red or 200 μM SKF-96365. Currents were sampled at 10 kHz and filtered at 3 kHz. The histogram of current amplitudes for each record is shown to the right. MS channel current-voltage relations measured in the presence of physiological saline (control) or physiological saline containing 1000 μM 2-APB, 40 μM ruthenium red or 200 μM SKF-96365. The single-channel conductance was obtained by a least squares fit to the data points with slope conductances of 22 pS, control, 2-APB, spermidine, flufenamic acid; 15.6 pS, 200 μM SKF-96365 and 11.4 pS, 40 μM ruthenium red.

TRPA1 and TRPP2.[12] Skeletal muscle expresses TRPC, TRPV and TRPM proteins.[13] There is evidence that TRPC1 is the MS channel in vertebrate cells[14] and that TRPC1 contributes to $Ca^{2+}$ entry in *mdx* muscle.[15,16] The importance of TRPC1 in the dystrophic process is further supported by studies showing expression levels are higher in *mdx* muscle with greater signs of damage.[17] In addition, muscle from *mdx* mice with a dominant negative TRPC transgene show reduced $Ca^{2+}$ entry and less severe dystrophy[18] and muscle from TRPC1 knockout mice show less contraction-induced injury than wild-type muscle.[19] On the other hand, several studies show TRPV2 and TRPV4 contribute to $Ca^{2+}$ entry and stretch-induced injury in *mdx* muscle.[16,20] Evidently, the precise molecular identity of the MS channel responsible for $Ca^{2+}$ entry in dystrophic skeletal muscle remains uncertain.

In this paper, we used patch clamp recording methods to study the block of MS channels by TRP channel antagonists at the level of single-channels. Our goal was to compare the pharmacological properties of the MS channels in skeletal muscle with the known pharmacological properties of recombinant TRP channel proteins. We find activators and inhibitors of TRPC channels have no effect on the activity of single MS channels recorded from membrane patches. By contrast, the TRPV antagonists, ruthenium red and SKF-96365, strongly block MS channels in skeletal muscle. Our results suggest MS channels in skeletal muscle have pharmacological properties that resemble TRPV channels. Other experiments showed an absence of MS channel activity in muscle from TRPV4 knockout mice and MS channel activation by hypotonic extracellular solutions. Together, these results suggest TRPV4 contributes to MS channels in skeletal muscle.

## Results

To test whether TRPC contributes to the MS channel in skeletal muscle, we exposed membrane patches to 1-oleoyl-2-acetyl-sn-glycerol (OAG, 100–200 μM) while recording single-channel activity. OAG activates TRPC1 and 3 channels in native and recombinant systems[22-24] and TRPC4,6,7.[25,26] Exposure of membrane patches to OAG added to the patch electrode had no effect on the activity of MS channel activity recorded from cell-attached patches (25/25 patches, data not shown). OAG also had no detectable effects on single-channel activity when added directly to the bathing solution. The absence of an effect of OAG suggests the skeletal muscle MS channel is not composed of TRPC subunits.

**Figure 1** shows the effects of a variety of TRP channel antagonists on the activity of single MS ion channels. Two aminoethoxydiphenyl borate (2-APB) blocks recombinant TRPC channels at low micromolar concentrations.[26-29] In our recordings from membrane patches, 2-APB produced no discernible effect on MS channel activity in skeletal muscle at concentrations up to 1 mM in the electrode solution. The record at the top of **Figure 1** shows a MS channel activity recorded in the presence of 500 μM 2-APB. The graph to the right of the figure is the distribution of current amplitudes plotted with the amplitude shown on the vertical axis. The record was obtained at a holding potential of –60 mV. At this potential, peak inward current was approximately 1.5–1.7 pA under control conditions in the absence of any blocker. The presence of 500 μM 2-APB had no effect on either the amplitude of the single-channel current nor on the apparent gating of the single channel over a wide range of concentrations. **Figure 1** also shows that 200 μM of either spermidine or flufenamic acid had little effect on the activity of single MS channels. By contrast, **Figure 1** shows that SKF-96365 and ruthenium red blocked the single-channel current. Block appeared as both a reduction in the amplitude of the single-channel current and a change in the gating transitions that occur within the open channel. Subsequent experiments examined the mechanism of block of MS channels by SKF-96365 and ruthenium red in more detail.

**Figure 2** shows the effect of the concentration of SKF-96365 added to the patch electrode on the single-channel activity. With 25 μM SKF-96365 in the electrode, there were few closures within a channel opening, similar to the channel activity

recorded in the absence of blocker. The few brief closures in the presence of 25 μM SKF-96365 could represent channel blocking events or conformational transitions of the channel protein. At higher concentrations of SKF-96365, there was a clear dose-dependent increase in the number of rapid closings. Adding 100 μM to the electrode produced far more fast closures when compared with the record obtained with 50 μM SKF-96365. With 200 μM SKF-96365 in the electrode, flickery block of the open channel increased to a point where the amplitude of the unitary current was difficult to discern. These observations suggest a simple model in which SKF-96365 acts as an open channel blocker in which the open and closed times represent the entry and exit of the drug from the channel pore.[30,31] The predictions of the open channel block model were tested in the next set of experiments.

**Figure 3** shows the analysis of the block of single MS channels in skeletal muscle by SKF-96365. **Figure 3A and B** shows the distribution of open and closed times within a single activation of the channel in the presence of either 50 μM (A) or 100 μM (B) SKF-9635 in the patch recording electrode. The histograms of open and closed times were fit with a single exponential, consistent with the presence of a single open and single closed state. **Figure 3C** shows the inverse of the mean open time (blocking rate) plotted as a function of the concentration of SKF-96365 in the patch electrode. The inverse of the mean open time increased with concentration of SKF-96365 in the electrode. As predicted by a simple two-state blocking model, the blocking rate depended linearly on the concentration of SKF-96365.

The slope of the relation between the inverse of the mean open time and the concentration of SKF-96365 gave a second-order rate coefficient $k_{on}$ = 13.3x10$^6$ M$^{-1}$s$^{-1}$. As shown in **Figure 3D**, the brief closed times (unblocking rate) decreased somewhat with increasing concentration of blocker. However, resolution of rapid closures was difficult and there was considerable scatter in the measured values of blocked times. A linear fit to the data gave mean blocked time $k_{off}$ = 1609 sec$^{-1}$. This value is not precise as there was considerable variability in the measured durations of blocked time, particularly at lower blocker concentrations where channel closing events outnumber blockages. The ratio of unblocking and blocking rates, $k_{off}/k_{on}$, gives a dissociation constant $K_D$ = ~124 μM. The results support the interpretation that SKF-96365 produces the rapid transitions between open and closed channel levels by acting as an open channel blocker in which it rapidly enters and exits the channel pore.

In the next set of experiments, we examined the blocking actions of ruthenium red on MS channel in skeletal muscle. **Figure 4** shows records of MS channel activity in the presence of different concentrations of ruthenium red. Ruthenium red had complex effects on the single-channel current. Increasing the concentration of ruthenium red from 5 μM (top record) to 40 μM (bottom record) clearly reduced the amplitude of the single-channel current. The amplitude of the single-channel current, however, was not constant but varied between several distinct levels. We interpreted this as ruthenium red causing a change in the probability of occupancy of the subconductance levels.

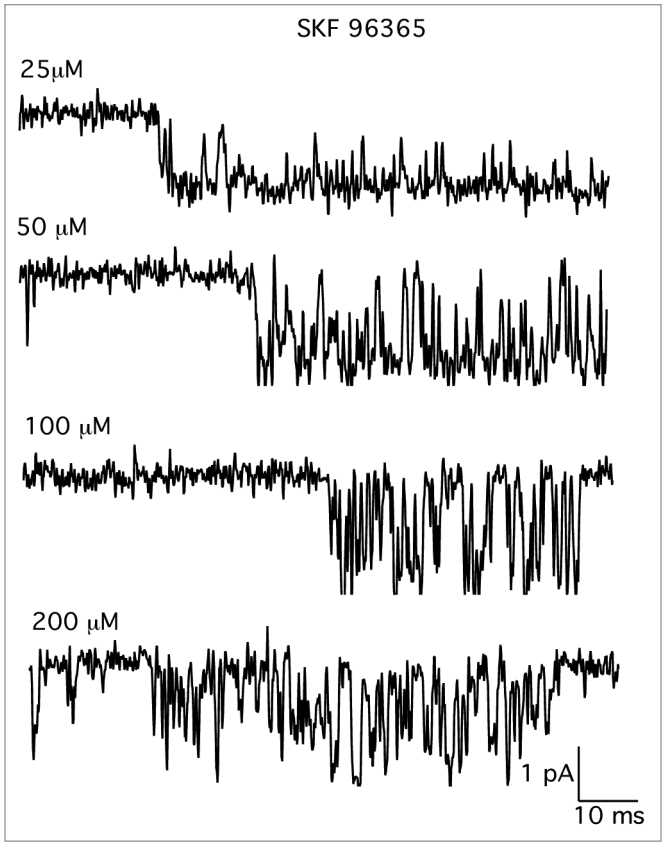


**Figure 2.** Records of single MS channel currents in the presence of increasing concentrations of SKF-96365. Records show single MS channel currents recorded in the presence of increasing concentrations of SKF-96365. SKF-96365 was added directly to the patch electrode filling solution. Each record is from a different patch. The holding potential was –60 Mv. Currents were digitized at 10 kHz and filtered at 3 kHz.

The effects of ruthenium red on MS channels resemble the block of MS channels by aminoglycoside antibiotics, in which blocker reduced both the amplitude of the single-channel current and increased occupancy of a subconductance level.[32] Block differed, however, in that aminoglycosides cause channels to fluctuate between the fully open state and a single subconductance level. By contrast, gating in the presence of ruthenium red appeared to involve transitions between several subconductance levels. We analyzed the subconductance behavior in the presence of ruthenium red by analyzing the distribution of current amplitudes open channel current, excluding all transitions to the fully closed state. The results of this analysis are shown in **Figure 5**.

**Figure 5A** shows single-channel currents recorded in the presence of either 10 μM (left) or 40 μM (right) ruthenium red. In the presence of 40 μM ruthenium red, the single-channel current is reduced, but the open channel current varies between several levels. We formed histograms of the amplitude of the open channel current by setting cursors within a channel opening event that excluded transitions to the fully closed, zero current level. Data points for the histograms were obtained from multiple channel openings within an experiment. The distribution of the amplitudes of the open channel current were skewed and could not be

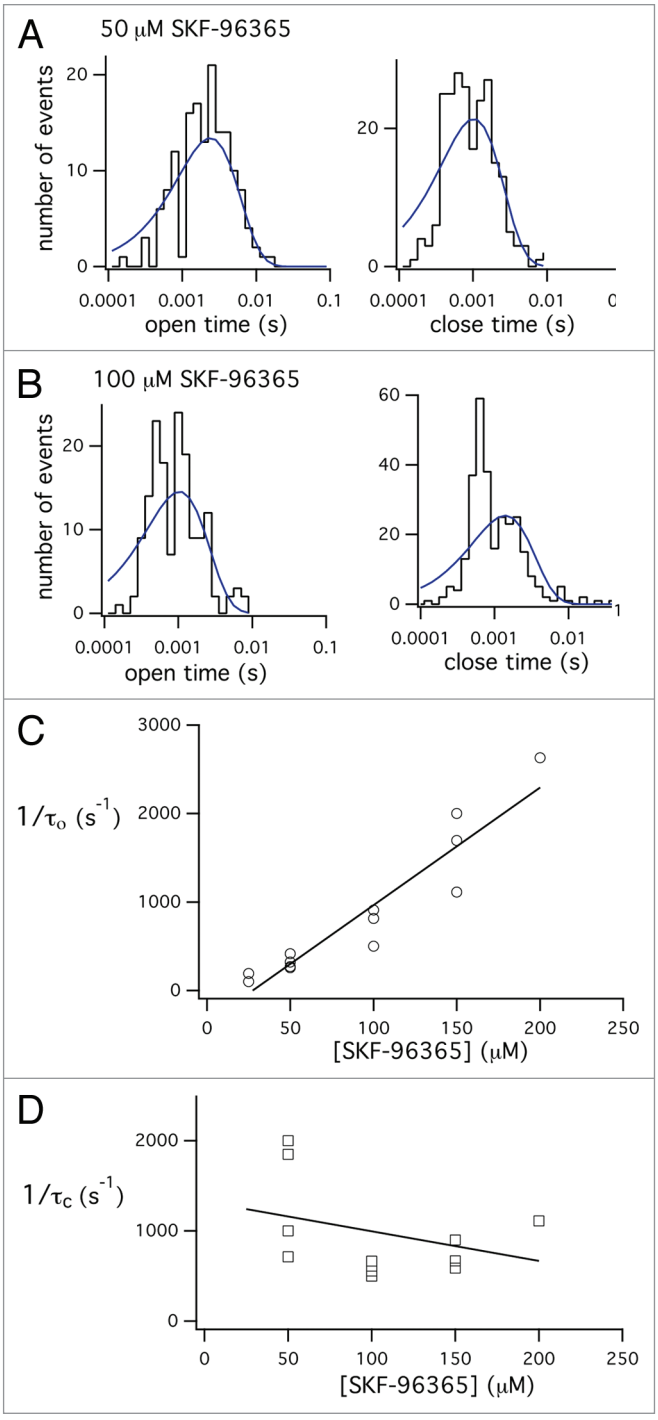


**Figure 3.** Analysis of the effect SKF-96365 on the mean open and closed times within a single opening. Histograms of open and closed times measured from records of single-channel activity recorded in the presence of either 50 μM (**A**) or 100 μM (**B**) SKF-96365. The histograms of open and closed times were fit with a single exponential function. (**C**) Plot of the reciprocal of the mean open time obtained from the single exponential fit to the open time distribution as a function of the concentration of SKF-96365 in the electrode. The data were fit with a straight line with slope = 13.3 and y-intercept –363.5, $r^2 = 0.9$. The fit was not constrained to go through zero, so the negative y-intercept is an artifact of the variability of the resolution of the open time measurements. (**D**) Plot of the reciprocal of the mean blocked times obtained from the single exponential fit of the closed time histogram. Data points obtained in the presence of 25 μM SKF-96365 were omitted from the plot, since at low concentrations of blocker the number of true channel closures far exceeds the number of blockages. The data were fit with a straight line with slope = -5.4 and y-intercept of 1608.7, $r^2 = 0.3$, indicating little dependence of blocked time on blocker concentration.

fit with a single Gaussian, as would be expected for a single open state with constant conductance. The skew can be seen in **Figure 5A** for the amplitude distribution for single-channel activity with 10 μM ruthenium red, where there is a "tail" extending toward zero current. We chose to fit the amplitude distribution of the open channel current as a sum of three Gaussian components, representing the fully open state (O) and two subconductance levels (S1 and S2). These levels are indicated with dotted lines in the records of single-channel activity. The fit to a sum of three Gaussian components was made using a maximum likelihood fitting routine.

**Figure 5B** shows that increasing the concentration of ruthenium red from 10–40 μM, reduced both the amplitude of the fully open state O as well as the probability of being in O, which was measured as the integral of the single Gaussian fit to O divided by the total area. We measured the distribution of current amplitudes for a number of experiments in which the patch electrode contained either 10, 15, 20 or 40 μM ruthenium red, as shown on the x-axis of **Figure 5B**. **Figure 5B** shows a plot of the probability of occupancy of O and the subconductance levels (S1 and S2) as a function of the ruthenium red concentration. The data shows that occupancy of state O decreases with blocker concentration, while there is an increase in the occupancy of S1 and S2. **Figure 5B** (inset) shows the amplitude of the fully open state plotted as a function of ruthenium red concentration. The fit data were fit with a simple expression for binding to a single site with a $K_{1/2}$ of 49 μM. These results show ruthenium red blocks MS channels by both reducing occupancy probability of state O with increased probability of S1 and S2 as well as reducing the amplitude of the fully open state. Similar behavior has been observed for the block of MS channels by aminoglycoside antibiotics.[32] Ruthenium red differs from aminoglycosides, such as neomycin, in having a greater potency (~49 μM vs. 200–300 μM, respectively. Thus, ruthenium red is a high affinity antagonist for MS channels in skeletal muscle.

**Figure 6** shows that subconductance fluctuations in the presence of ruthenium red depend on membrane potential. In this experiment, the patch electrode contained 20 μM ruthenium red. Single channel activity was recorded at a constant holding potential of either –70, -50 or –30 mV. The amplitude distributions of the open channel current were obtained at each holding potential and the distribution fit as the sum of three Gaussian components. Inspection of the amplitude distributions measured at each voltage in the presence of a constant concentration of ruthenium red shows progressive reduction in the occupancy of the fully open state O, with a corresponding increase in occupancy of the next sublevel, S1. The results suggest subconductance fluctuations produced by ruthenium red are voltage-dependent and likely contribute to the blocking mechanism at depolarized membrane potentials. Further studies are required to analyze the precise

mechanism of block of MS channels by ruthenium red in skeletal muscle and are not considered further in this paper.

The pharmacological analysis shows MS channels in skeletal muscle are insensitive to 2-APB, but blocked by SKF-96365 and ruthenium red, properties consistent with TRPV channels. The absence of a potentiating effect of 2-APB on MS channels suggests MS channels are not TRPV1, 2 or 3. A possible candidate is TRPV4, which shows mechanosensitive gating in mammalian cells.[33,34] In addition, TRPV4 knockout mice have reduced sensitivity to pressure stimuli,[33] central osmoreception,[35] and minor abnormalities in auditory processing,[36] but are otherwise phenotypically normal. The defects in various forms of mechanosensation in the TRPV4 knockout suggests TRPV4 may function as a mechanosensitive ion channel. We recorded single-channel activity from skeletal muscle fibers from TRPV4 knockout mice to test the hypothesis TRPV4 contributes to MS channels.

FDB fibers were isolated from TRPV4 knockout mice and single-channel activity recorded from membrane patches. Recordings were made with physiological saline in the patch electrode at a holding potential of –60 mV. Patch currents were recorded for 1–5 min at –60 mV and then the holding potential was changed in 10 mV increments from –60 to –10 mV. We recorded patch currents at each holding potential for 1–3 min. MS channel open probability increases with depolarization[6,7] and so recordings at potentials more positive than –60 would increase the likelihood of observing channel activity. Despite the long recording times at both negative and more depolarized voltages, we failed to detect either spontaneous MS channel activity or activity induced by applying suction to the patch electrode in 21 out of 21 recordings from membrane patches on FDB fibers from TRPV4$^{-/-}$ mice. Previous work shows ~70% of recordings from membrane patches on wild-type FDB fibers show robust MS channel activity.[7] Therefore, the probability of observing no MS channel activity in our experiments if channels were present is negligibly small.

Vriens et al. showed that hypotonic solutions activate TRPV4 in response to cell swelling.[34] Skeletal muscle fiber volume increases linearly with the inverse of the extracellular osmotic strength over the range 77–1100 mOsms, indicating fibers behave as a freely distensible, semipermeable bag containing a fixed amount of solute.[37] There is evidence hypotonic solutions increase single channel activity in normal and dystrophic human myotubes.[38] Therefore, we performed experiments examining the effects of hypotonic solutions on the activity of single MS channels in skeletal muscle.

**Figure** 7 shows an example of an experiment where the normal extracellular solution was switched to a hypotonic solution (250 mOsms). In these experiments, muscle fibers were exposed to the hypotonic solution while recording from membrane patches. **Figure** 7 shows reducing the osmolarity from 350–250 mOsms was associated with the appearance of a 25 pS channel. In this experiment, the channel showed prolonged open times, consistent with a hypo-osmotic activation mechanism. This behavior was observed in 3 out of 10 patches. In some of the experiments, exposure to a hypotonic solution was associated with the appearance of a larger conductance channel of ~35–38 pS (data not shown). The results suggest that MS channels may be activated by hypotonic solutions.

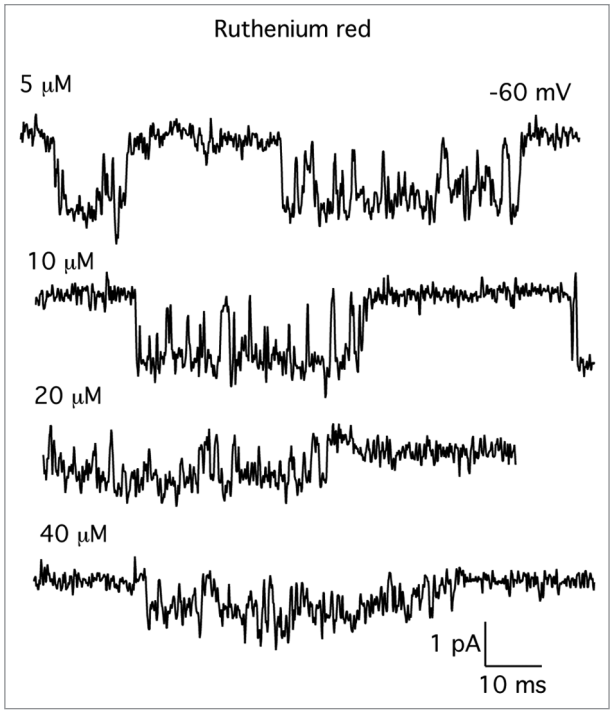


**Figure 4.** Records of single MS channel currents in the presence of increasing concentrations of ruthenium red. Ruthenium red was added directly to the patch electrode filling solution. Each record is from a different patch. The concentration of ruthenium red is indicated by each record. The holding potential was –60 mV. Currents were digitized at 10 kHz and filtered at 3 kHz.

## Discussion

The main finding of this paper is that ruthenium red blocks MS channels in mouse skeletal muscle with relatively high affinity ($K_{1/2}$ = 49 μM). SKF-96365 also blocks MS channels, but with lower potency ($K_D$ = ~129 μM). Block of MS channels by SKF-96365 follows the predictions of a simple open channel blocking model: mean open and closed times are exponentially distributed; the inverse of the mean open time depends linearly on concentration; the inverse of the mean blocked times is independent of blocker concentration. Ruthenium red, by contrast, has a more complex blocking mechanism, involving both a reduction in the amplitude of the single-channel current and occupancy of subconductance levels. In contrast to the relatively high affinity block of MS channels produced by ruthenium red and SKF-96365, we find 2-APB, flufenamic acid, and spermidine have little or no effect on the single-channel currents up to concentrations approaching one millimolar. In the discussion below, we first compare the biophysical and pharmacological properties of MS channels with those of recombinant TRP channels. We then discuss our results in relation to previous studies of the role of TRP channels in $Ca^{2+}$ entry in normal and dystrophic muscle.

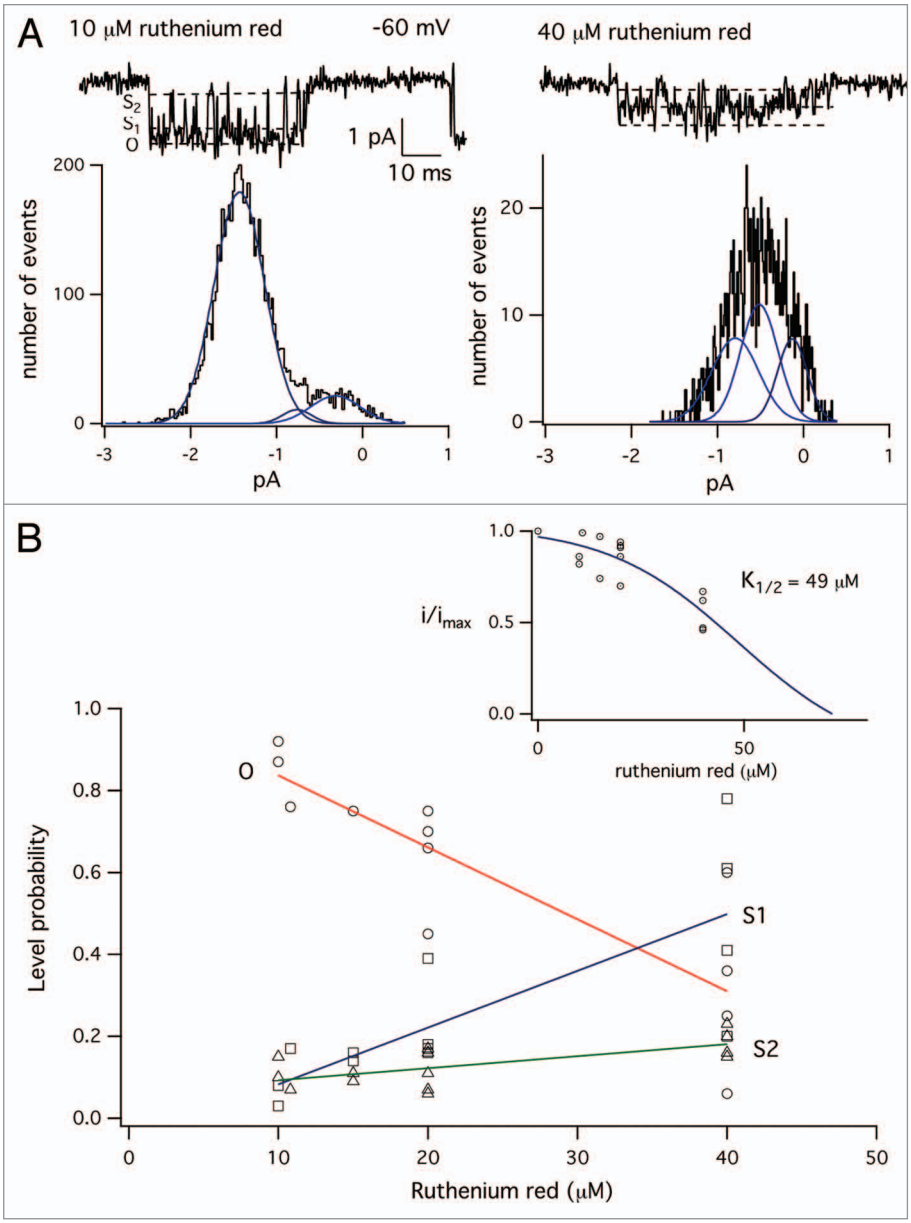


**Figure 5.** Analysis of the effect of ruthenium red on the amplitude of the single-channel current. (**A**) Single channel currents recorded in the presence of either 10 μM (left) or 40 μM (right) ruthenium red. The graph below each single-channel current shows the amplitude distribution of open channel current. Histograms were constructed by including data points from 5–20 channel openings during an experiment, excluding periods when the channel closed to the zero current level. The amplitude distributions were fit as the sum of three Gaussian components by a maximum likelihood fitting routine. (**B**) Plot of the occupancy probability of the fully open state, O and subconductance states S1 and S2. Occupancy probabilities were measured as the integral of each Gaussian component divided by the total area under all three curves. Data were fit straight line by linear regression. (Inset) Plot of the amplitude of the fully open state, O, as a function of ruthenium red concentration in the patch electrode. The data were fit with a simple expression for binding to a single site, with $K_{1/2}$ = 49 μM.

MS channels in skeletal muscle share certain biophysical properties with TRPV channels. For example, MS channels in skeletal muscle have a $Ca^{2+}$ permeability, $P_{Ca}{}^{2+}/P_{K+}$ = ~7.[39] The $Ca^{2+}$ permeability is within the range of 1–10 measured for TRPV1, 2, 3 and 4.[40] In addition, MS channels have a monovalent cation selectivity sequence (Rb > K > Na > Cs > Li)[6] that corresponds to Eisenman sequence III, indicating an ion binding site with a relatively weak field-strength. This sequence is quite similar to TRPV4, which has a cation selectivity sequence corresponding to Eisenman sequence IV, and also a weak field-strength binding site.[41] In addition, MS channels in skeletal muscle are very sensitive to block by the lanthanide cation, $Gd^{3+}$: $Gd^{3+}$ blocks both stretch-activated and stretch-inactivated MS channels in normal and *mdx* muscle with virtually identical affinities ($K_D$ = ~6 μM).[6,42] The high affinity block by $Gd^{3+}$ is similar to that reported for TRPV4 (~1 μM).[41]

2-APB strongly activates current through TRPV1, 2 and 3 channels.[43,44] The absence of facilitation of MS channel activity by 2-APB in this study suggests TRPV1, 2 and 3 do not contribute to the MS channels in skeletal muscle. We cannot, however, rule out there are 2-APB-insensitive TRPV1, 2 or 3 variants in skeletal muscle. This possibility is suggested by the finding that a recombinant human TRPV2 channel is insensitive to 2-APB.[45] TRPV2 is highly expressed in skeletal muscle where it resides in an intracellular compartment and translocates to the sarcolemma in response to membrane stretch.[46] However, the blocking potencies of ruthenium red and SKF-96365 for recombinant TRPV2 channels ($EC_{50}$ = 7 and 21 μM, respectively) are somewhat greater than their potency in blocking MS channels ($K_D$ = ~49 and 147 μM).[45] Taken together, the results suggest MS channels in skeletal muscle are not TRPV2. In support of this interpretation, we failed to observe an effect of elevated temperature (~45°C) on single MS channels in skeletal muscle (unpublished data).

The biophysical properties of MS channels also differ considerably from TRPM, since MS channels are relatively insensitive to changes in extracellular pH[32] and intracellular $Mg^{2+}$ (unpublished data). In addition, we find flufenamic acid failed to inhibit MS channels in muscle (**Fig. 1**), although one study found that it inhibits recombinant TRPM2 and 3 in a heterologous expression system.[47] This same study found a relatively potent block of TRPV4 channels by flufenamic acid ($EC_{50}$ = ~41 μM).[47] However, this experiment used calcium imaging in TRPV4 transfected cells and the blocking actions of

flufenamic acid on intracellular calcium signals may be more difficult to interpret than direct electrophysiological recordings of single-channel activity.

The available data lead us to conclude TRPV4 is a likely candidate for the MS channel in skeletal muscle. Recordings of single-channel activity provide direct information on the pharmacological properties of MS channels. The results, however, are limited in that more extensive electrophysiological experiments are necessary to investigate a much wider range of TRPV4 activators and inhibitors. Nonetheless, activation of MS channels by hypotonic extracellular solutions and the absence of MS channel activity in muscle from TRPV4 knockout mice suggests TRPV4 contributes to the MS channel in skeletal muscle.

On the other hand, single-channel recordings from muscle isolated from TRPC1 knockout mice show the absence of a mechanically-insensitive, small conductance channel. Zanou et al. also reported activity of a larger conductance channel in the TRPC1 knockout.[16] The properties of the large conductance channel, however, were not studied. In particular, its response to mechanical stimulation was not described. Nonetheless, these results suggest TRPC1 is not the mechanosensitive channel in muscle. Despite this conclusion, there is good evidence for a role of TRPC1 in $Ca^{2+}$ entry and muscle damage in normal and dystrophic muscle from *mdx* mice.[17-19]

These observations for a functional role of TRPC1 in the pathogenesis of dystrophin-deficiency suggest either TRPC1 acts as an independent source of $Ca^{2+}$ entry contributing to the dystrophic phenotype or that MS channels represent a novel variant formed by heteromeric subunit assembly TRPV4 subunits.[48,49] Ma et al. showed TRPV4 and TRPC1 coassemble to form heteromeric TRPV4-C1 channels.[50] The properties of these channels, however, are different from MS channels in having a much larger single-channel conductance (~83 pS) and a cation selectivity sequence corresponding to a strong, rather than weak, field-strength cation binding site. In addition, TRPP2 has been shown to form a heterotetramer with TRPV4.[51] The possibility that MS channels exist as heteromeric proteins containing TRPV4 and other TRP channel subunits remains to be tested.

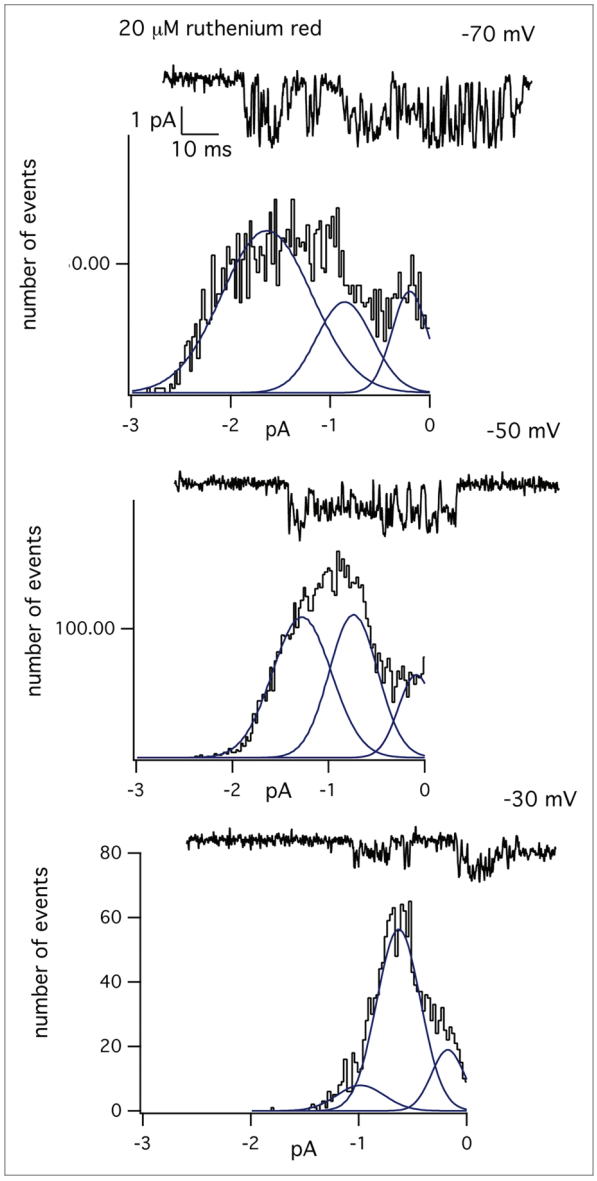


**Figure 6.** Voltage-dependence of the subconductance transitions in the presence of ruthenium red. Experiment showing the block of the single-channel current produced by 20 μM ruthenium red at a constant holding potential of either –70, –50 or –30 Mv. The graph below each record is the amplitude distribution of the open channel current measured at the indicated membrane potential. Each amplitude distribution was fit with the sum of three Gaussian components using a maximum likelihood fitting routine.

## Materials and Methods

Methods for isolation of skeletal muscle fibers from mice and general electrophysiological methods are identical to those described in previous studies.[7,21] Wild-type mice (C57BL) were obtained from a local supplier. TRPV4 knockout mice were generously provided by Dr. Nigel Bunnett (UCSF). Mice were sacrificed after isoflurane anesthesia according to a protocol approved by the UCSF Committee on Animal Research. Single muscle fibers were isolated from the *flexor digitorum brevis* following treatment of an isolated muscle bundle with 0.25% collagenase B (Worthington Biochemical) in DMEM-H16 medium for 20 min. The treated muscle was rinsed in DMEM-H16 containing 0.5% horse serum and single fibers dispersed by passing the muscle bundle through the tip of a heat-polished Pasteur pipette. Dissociated single fibers were placed on a glass coverslip forming the bottom of an experimental chamber that was attached to the stage of an inverted microscope. Electrophysiological recordings were made from intact cells that adhered to the glass coverslip.

Patch electrodes were pulled in two stages from borosilicate capillaries (Custom 8520, Warner Instruments), coated with Sylgard® (Dow Corning) near the tips, and heat polished to give a final resistance of 2–4 MΩ when filed with a physiological saline solution and immersed in an isotonic $K^+$-aspartate bathing solution. Single-channel currents were recorded with an EPC-9 patch clamp amplifier (HEKA Instruments) using Pulse® (HEKA) software for stimulus generation and data acquisition.

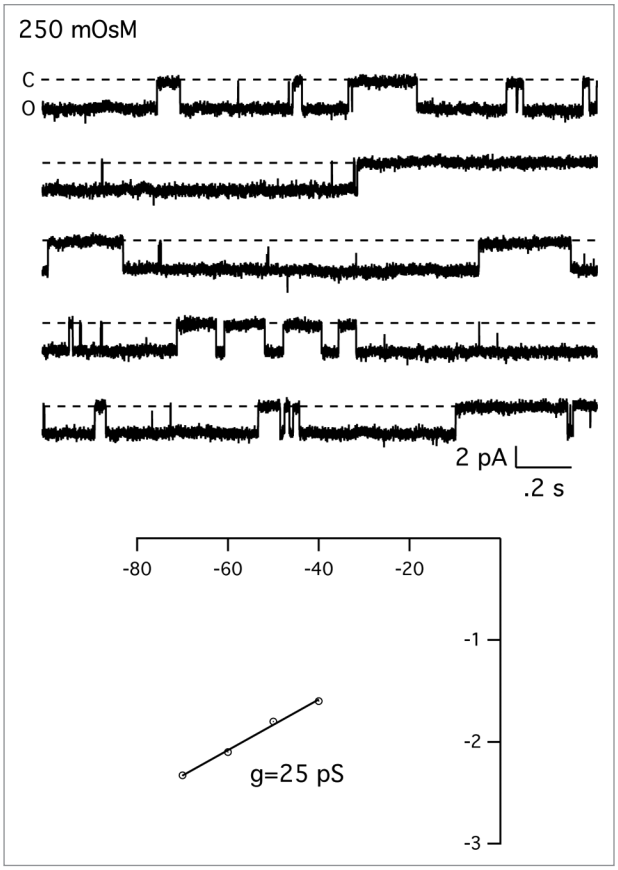


**Figure 7.** Hypo-osmotic activation of the MS channel in skeletal muscle. Experiment showing the effect of hypotonic solution on MS channels in skeletal muscle fibers. Recordings was made from a cell-attached patch and the extracellular solution (345 mOsm) replaced with a dilute extracellular solution (250 mOsm). There was no channel activity prior to exposure of the cell to the hypotonic solution. Currents were digitized at 2.5 Khz and filtered at 500 Hz. Bottom shows the single-channel current-voltage relationship.

Currents were digitized at either 2.5 or 10 kHz, filtered at 0.5 or 3 kHz, and stored directly on the hard disk of a Power Mac G4. Digitized currents were exported into IgorPro® (Wavemetrics) or TAC® (Bruxton Corporation) for analysis.

The electrode solution contained (in millimolar) 150 NaCl, 5 KCl, 1 $MgCl_2$, 10 EGTA, 10 HEPES and 17 glucose. The pH was adjusted to 7.45 by adding tetraethylammonium hydroxide (TEA-OH). The isotonic $K^+$ bathing solution contained (in millimolar) 150 potassium aspartate, 5 $MgCl_2$, 10 EGTA, 10 HEPES and 10 glucose. The pH was adjusted to 7.45 with TEA-OH. The high $K^+$ bathing solution was used to zero the cell's membrane potential so the patch potential would be the same as the voltage command. Excision of the membrane patch from the cell at the end of an experiment indicated voltage error < 5 mV. Experiments in which the electrode potential drifted by more than 5 mV at the end of an experiment were not used for analysis.

The drugs, 2-aminoethoxydiphenyl borate (2-APB), ruthenium red, SKF-96365, and 1-oleolyl-2-acetyl-sn-glycerol (OAG) were obtained from Sigma-Aldrich. 2-APB and OAG were prepared as a concentrated stock solutions in dimethyl sulfoxide (DMSO) which was diluted with the experimental saline solution to give the final desired concentration. The concentration of DMSO in the experimental solutions was < 1%. In these experiments, drugs were added directly to the patch electrode filling solution. Drug solutions were prepared freshly on the day of the experiment.

### Disclosure of Potential Conflicts of Interest

No potential conflicts of interest were disclosed.



### References


1. Hamill OP, Martinac B. Molecular basis of mechanotransduction in living cells. Physiol Rev 2001; 81:685-740; PMID:11274342.
2. Jaalouk DE, Lammerding J. Mechanotransduction gone awry. Nat Rev Mol Cell Biol 2009; 10:63-73; PMID:19197333; http://dx.doi.org/10.1038/nrm2597.
3. Blake DJ, Weir A, Newey SE, Davies KE. Function and genetics of dystrophin and dystrophin-related proteins in muscle. Physiol Rev 2002; 82:291-329; PMID:11917091.
4. Tanabe Y, Esaki K, Nomura T. Skeletal muscle pathology in X chromosome-linked muscular dystrophy (mdx) mouse. Acta Neuropathol 1986; 69:91-5; PMID:3962599; http://dx.doi.org/10.1007/BF00687043.
5. Carnwath JW, Shotton DM. Muscular dystrophy in the mdx mouse: histopathology of the soleus and extensor digitorum longus muscles. J Neurol Sci 1987; 80:39-54; PMID:3612180; http://dx.doi.org/10.1016/0022-510X(87)90219-X.
6. Franco A Jr., Lansman JB. Stretch-sensitive channels in developing muscle cells from a mouse cell line. J Physiol 1990; 427:361-80; PMID:2170636.
7. Franco-Obregón A Jr., Lansman JB. Mechanosensitive ion channels in skeletal muscle from normal and dystrophic mice. J Physiol 1994; 481:299-309; PMID:7537813.
8. Lansman JB, Franco-Obregón A. Mechanosensitive ion channels in skeletal muscle: a link in the membrane pathology of muscular dystrophy. Clin Exp Pharmacol Physiol 2006; 33:649-56; PMID:16789935; http://dx.doi.org/10.1111/j.1440-1681.2006.04393.x.
9. Lansman JB. Mechanosensitive ion channels in dystrophic muscle. In: Hamill OP, ed. Current Topics in Membranes Volume 59: Mechanosensitive Ion Channels, Part B. Elsevier Inc, 2007:467-484.
10. Yeung EW, Whitehead NP, Suchyna TM, Gottlieb PA, Sachs F, Allen DG. Effects of stretch-activated channel blockers on $[Ca^{2+}]_i$ and muscle damage in the mdx mouse. J Physiol 2005; 562:367-80; PMID:15528244; http://dx.doi.org/10.1113/jphysiol.2004.075275.
11. Whitehead NP, Yeung EW, Allen DG. Muscle damage in mdx (dystrophic) mice: role of calcium and reactive oxygen species. Clin Exp Pharmacol Physiol 2006; 33:657-62; PMID:16789936; http://dx.doi.org/10.1111/j.1440-1681.2006.04394.x.
12. Arnadóttir J, Chalfie M. Eukaryotic mechanosensitive channels. Annu Rev Biophys 2010; 39:111-37; PMID:20192782; http://dx.doi.org/10.1146/annurev.biophys.37.032807.125836.
13. Brinkmeier H. TRP channels in skeletal muscle: gene expression, function and implications for disease. Adv Exp Med Biol 2011; 704:749-58; PMID:21290325; http://dx.doi.org/10.1007/978-94-007-0265-3_39.
14. Maroto R, Raso A, Wood TG, Kurosky A, Martinac B, Hamill OP. TRPC1 forms the stretch-activated cation channel in vertebrate cells. Nat Cell Biol 2005; 7:179-85; PMID:15665854; http://dx.doi.org/10.1038/ncb1218.
15. Vandebrouck C, Martin D, Colson-Van Schoor M, Debaix H, Gailly P. Involvement of TRPC in the abnormal calcium influx observed in dystrophic (mdx) mouse skeletal muscle fibers. J Cell Biol 2002; 158:1089-96; PMID:12235126; http://dx.doi.org/10.1083/jcb.200203091.
16. Zanou N, Shapovalov G, Louis M, Tajeddine N, Gallo C, Van Schoor M, et al. Role of TRPC1 channel in skeletal muscle function. Am J Physiol Cell Physiol 2010; 298:C149-62; PMID:19846750; http://dx.doi.org/10.1152/ajpcell.00241.2009.
17. Matsumura CY, Taniguti AP, Pertille A, Santo Neto H, Marques MJ. Stretch-activated calcium channel protein TRPC1 is correlated with the different degrees of the dystrophic phenotype in mdx mice. Am J Physiol Cell Physiol 2011; 301:C1344-50; PMID:21900691; http://dx.doi.org/10.1152/ajpcell.00056.2011.

18. Millay DP, Goonasekera SA, Sargent MA, Maillet M, Aronow BJ, Molkentin JD. Calcium influx is sufficient to induce muscular dystrophy through a TRPC-dependent mechanism. Proc Natl Acad Sci USA 2009; 106:19023-8; PMID:19864620; http://dx.doi.org/10.1073/pnas.0906591106.
19. Zhang BT, Whitehead NP, Gervasio OL, Reardon TF, Vale M, Fatkin D, et al. Pathways of Ca2+ entry and cytoskeletal damage following eccentric contractions in mouse skeletal muscle. J Appl Physiol 2012; 112:2077-86; PMID:22461447; http://dx.doi.org/10.1152/japplphysiol.00770.2011.
20. Pritschow BW, Lange T, Kasch J, Kunert-Keil C, Liedtke W, Brinkmeier H. Functional TRPV4 channels are expressed in mouse skeletal muscle and can modulate resting $Ca^{2+}$ influx and muscle fatigue. Pflugers Arch 2011; 461:115-22; PMID:20924600; http://dx.doi.org/10.1007/s00424-010-0883-4.
21. Franco-Obregón A, Lansman JB. Changes in mechanosensitive channel gating following mechanical stimulation in skeletal muscle myotubes from the mdx mouse. J Physiol 2002; 539:391-407; PMID:11882673; http://dx.doi.org/10.1113/jphysiol.2001.013043.
22. Lintschinger B, Balzer-Geldsetzer M, Baskaran T, Graier WF, Romanin C, Zhu MX, et al. Coassembly of Trp1 and Trp3 proteins generates diacylglycerol- and $Ca^{2+}$-sensitive cation channels. J Biol Chem 2000; 275:27799-805; PMID:10882720.
23. Venkatachalam K, Zheng F, Gill DL. Regulation of canonical transient receptor potential (TRPC) channel function by diacylglycerol and protein kinase C. J Biol Chem 2003; 278:29031-40; PMID:12721302; http://dx.doi.org/10.1074/jbc.M302751200.
24. Liu X, Bandyopadhyay BC, Singh BB, Groschner K, Ambudkar IS. Molecular analysis of a store-operated and 2-acetyl-sn-glycerol-sensitive non-selective cation channel. Heteromeric assembly of TRPC1-TRPC3. J Biol Chem 2005; 280:21600-6; PMID:15834157; http://dx.doi.org/10.1074/jbc.C400492200.
25. Estacion M, Li S, Sinkins WG, Gosling M, Bahra P, Poll C, et al. Activation of human TRPC6 channels by receptor stimulation. J Biol Chem 2004; 279:22047-56; PMID:15023993; http://dx.doi.org/10.1074/jbc.M402320200.
26. Zagranichnaya TK, Wu X, Villereal ML. Endogenous TRPC1, TRPC3, and TRPC7 proteins combine to form native store-operated channels in HEK-293 cells. J Biol Chem 2005; 280:29559-69; PMID:15972814; http://dx.doi.org/10.1074/jbc.M505842200.
27. Trebak M, Bird GS, McKay RR, Putney JW Jr. Comparison of human TRPC3 channels in receptor-activated and store-operated modes. Differential sensitivity to channel blockers suggests fundamental differences in channel composition. J Biol Chem 2002; 277:21617-23; PMID:11943785; http://dx.doi.org/10.1074/jbc.M202549200.
28. Lievremont JP, Bird GS, Putney JW Jr. Mechanism of inhibition of TRPC cation channels by 2-aminoethoxydiphenylborane. Mol Pharmacol 2005; 68:758-62; PMID:15933213.
29. Xu SZ, Zeng F, Boulay G, Grimm C, Harteneck C, Beech DJ. Block of TRPC5 channels by 2-aminoethoxydiphenyl borate: a differential, extracellular and voltage-dependent effect. Br J Pharmacol 2005; 145:405-14; PMID:15806115; http://dx.doi.org/10.1038/sj.bjp.0706197.
30. Neher E, Steinbach JH. Local anaesthetics transiently block currents through single acetylcholine-receptor channels. J Physiol 1978; 277:153-76; PMID:306437.
31. Lansman JB, Hess P, Tsien RW. Blockade of current through single calcium channels by Cd2+, Mg2+, and Ca2+. Voltage and concentration dependence of calcium entry into the pore. J Gen Physiol 1986; 88:321-47; PMID:2428920; http://dx.doi.org/10.1085/jgp.88.3.321.
32. Winegar BD, Haws CM, Lansman JB. Subconductance block of single mechanosensitive ion channels in skeletal muscle fibers by aminoglycoside antibiotics. J Gen Physiol 1996; 107:433-43; PMID:8868053; http://dx.doi.org/10.1085/jgp.107.3.433.
33. Suzuki M, Mizuno A, Kodaira K, Imai M. Impaired pressure sensation in mice lacking TRPV4. J Biol Chem 2003; 278:22664-8; PMID:12692122; http://dx.doi.org/10.1074/jbc.M302561200.
34. Vriens J, Watanabe H, Janssens A, Droogmans G, Voets T, Nilius B. Cell swelling, heat, and chemical agonists use distinct pathways for the activation of the cation channel TRPV4. Proc Natl Acad Sci U S A 2004; 101:396-401; PMID:14691263; http://dx.doi.org/10.1073/pnas.0303329101.
35. Mizuno A, Matsumoto N, Imai M, Suzuki M. Impaired osmotic sensation in mice lacking TRPV4. Am J Physiol Cell Physiol 2003; 285:C96-101; PMID:12777254.
36. Tabuchi K, Suzuki M, Mizuno A, Hara A. Hearing impairment in TRPV4 knockout mice. Neurosci Lett 2005; 382:304-8; PMID:15925108; http://dx.doi.org/10.1016/j.neulet.2005.03.035.
37. Blinks JR. Influence of osmotic strength on cross-section and volume of isolated single muscle fibers. J Physiol 1965; 177:42-57; PMID:14296959.
38. Vandebrouck C, Duport G, Raymond G, Cognard C. Hypotonic medium increases calcium permeant channels activity in human normal and dystrophic myotubes. Neurosci Lett 2002; 323:239-43; PMID:11959428; http://dx.doi.org/10.1016/S0304-3940(02)00148-9.
39. Franco A Jr., Lansman JB. Calcium entry through stretch-inactivated ion channels in mdx myotubes. Nature 1990; 344:670-3; PMID:1691450; http://dx.doi.org/10.1038/344670a0.
40. Owsianik G, Talavera K, Voets T, Nilius B. Permeation and selectivity of TRP channels. Annu Rev Physiol 2006; 68:685-717; PMID:16460288; http://dx.doi.org/10.1146/annurev.physiol.68.040204.101406.
41. Watanabe H, Davis JB, Smart D, Jerman JC, Smith GD, Hayes P, et al. Activation of TRPV4 channels (hVRL-2/mTRP12) by phorbol derivatives. J Biol Chem 2002; 277:13569-77; PMID:11827975; http://dx.doi.org/10.1074/jbc.M200062200.
42. Franco A Jr., Winegar BD, Lansman JB. Open channel block by gadolinium ion of the stretch-inactivated ion channel in mdx myotubes. Biophys J 1991; 59:1164-70; PMID:1714778; http://dx.doi.org/10.1016/S0006-3495(91)82332-3.
43. Hu HZ, Gu Q, Wang C, Colton CK, Tang J, Kinoshita-Kawada M, et al. 2-aminoethoxydiphenyl borate is a common activator of TRPV1, TRPV2, and TRPV3. J Biol Chem 2004; 279:35741-8; PMID:15194687; http://dx.doi.org/10.1074/jbc.M404164200.
44. Chung MK, Lee H, Mizuno A, Suzuki M, Caterina MJ. 2-aminoethoxydiphenyl borate activates and sensitizes the heat-gated ion channel TRPV3. J Neurosci 2004; 24:5177-82; PMID:15175387; http://dx.doi.org/10.1523/JNEUROSCI.0934-04.2004.
45. Juvin V, Penna A, Chemin J, Lin YL, Rassendren FA. Pharmacological characterization and molecular determinants of the activation of transient receptor potential V2 channel orthologs by 2-aminoethoxydiphenyl borate. Mol Pharmacol 2007; 72:1258-68; PMID:17673572; http://dx.doi.org/10.1124/mol.107.037044.
46. Iwata Y, Katanosaka Y, Arai Y, Komamura K, Miyatake K, Shigekawa M. A novel mechanism of myocyte degeneration involving the $Ca^{2+}$-permeable growth factor-regulated channel. J Cell Biol 2003; 161:957-67; PMID:12796481; http://dx.doi.org/10.1083/jcb.200301101.
47. Klose C, Straub I, Riehle M, Ranta F, Krautwurst D, Ullrich S, et al. Fenamates as TRP channel blockers: mefenamic acid selectively blocks TRPM3. Br J Pharmacol 2011; 162:1757-69; PMID:21198543; http://dx.doi.org/10.1111/j.1476-5381.2010.01186.x.
48. Hellwig N, Albrecht N, Harteneck C, Schultz G, Schaefer M. Homo- and heteromeric assembly of TRPV channel subunits. J Cell Sci 2005; 118:917-28; PMID:15713749; http://dx.doi.org/10.1242/jcs.01675.
49. Cheng W, Yang F, Takanishi CL, Zheng J. Thermosensitive TRPV channel subunits coassemble into heteromeric channels with intermediate conductance and gating properties. J Gen Physiol 2007; 129:191-207; PMID:17325193; http://dx.doi.org/10.1085/jgp.200709731.
50. Ma X, Nilius B, Wong JW, Huang Y, Yao X. Electrophysiological properties of heteromeric TRPV4-C1 channels. Biochim Biophys Acta 2011; 1808:2789-97; PMID:21871867; http://dx.doi.org/10.1016/j.bbamem.2011.07.049.
51. Stewart AP, Smith GD, Sandford RN, Edwardson JM. Atomic force microscopy reveals the alternating subunit arrangement of the TRPP2-TRPV4 heterotetramer. Biophys J 2010; 99:790-7; PMID:20682256; http://dx.doi.org/10.1016/j.bpj.2010.05.012.